



Epitaxial (La,Sr)TiO₃ as a conductive buffer for high temperature superconducting coated conductors

K. Kim^a, Y.W. Kwon^a, D.P. Norton^{a,*}, D.K. Christen^b, J.D. Budai^b,
B.C. Sales^b, M.F. Chisholm^b, C. Cantoni^b, K. Marken^c

^a Department of Materials Science and Engineering, University of Florida, 100 Rhines Hall, Gainesville, FL 32611, USA

^b Oak Ridge National Laboratory, Oak Ridge, TN 37831, USA

^c Oxford Superconducting Technology, 600 Milik street, Carteret, NJ 07008, USA

Received 12 September 2002; received in revised form 2 January 2003; accepted 3 February 2003

Abstract

The transport and structural properties of (La,Sr)TiO₃ epitaxial thin films grown by pulsed-laser deposition is presented. In particular, the potential use of (La,Sr)TiO₃ as a conductive buffer layer for subsequent growth of high temperature superconducting films for coated conductors is discussed. Van der Pauw measurements of film resistivity as a function of oxidation conditions show that, for undoped LaTiO₃ films, the resistivity increases rapidly as background oxygen pressure is increased, which is consistent with the formation of the LaTiO_{3+x} phase. Sr doping of LaTiO₃ significantly enhances the conductivity of thin film materials when synthesized under oxidizing conditions. The transport behavior for Sr-doped LaTiO₃ films correlates with structural data showing no significant shift in lattice spacing as oxygen partial pressure is increased during film growth. In addition, the epitaxial growth of (La,Sr)TiO₃ on biaxially textured Ni alloy tapes is demonstrated. These results suggest that (La,Sr)TiO₃ is a viable candidate as a conducting buffer for superconducting film growth on biaxially textured metal tapes.

© 2003 Elsevier Ltd. All rights reserved.

Keywords: Coated conductors; Wires; Epitaxial films; Buffer layers

In recent years, significant interest has emerged regarding the fundamental properties and application of conducting oxides [1–3]. Among the materials investigated is the (La,Sr)TiO₃ system [4–10]. LaTiO_{3+x} is a defect perovskite, with transport properties varying from insulating to metallic based on oxygen stoichiometry. LaTiO₃ is a Mott insulator with a G-type antiferromagnetic ordered ground state and a Néel temperature of approximately 135 K. At high temperature, LaTiO₃ is a semiconductor, becoming an antiferromagnetic insulator upon cooling through the Néel temperature. When synthesized with moderate oxygen

content, LaTiO_{3-x} is metallic at high temperature, with a metal-insulator transition occurring at reduced temperature. As oxygen is added, ordered phases are observed. For $0.1 < x < 0.2$, the material is metallic at all temperatures. As more oxygen is loaded into the lattice, intergrowths are introduced. At $x = 0.4$, the material again becomes a *p*-type semiconductor. For $x = 0.5$, the material becomes ferroelectric, assuming the monoclinic La₂Ti₂O₇ layered structure made of two regular perovskite units stacked between two distorted units that share an additional oxygen layer. La₂Ti₂O₇ exhibits a relatively high Curie temperature of 1773 K [11]. The saturation polarization is 5 μC/cm², and a coercive field of 45 kV/cm. Upon doping with Sr, bulk La_{1-x}Sr_xTiO₃ transforms from an antiferromagnetic *p*-type semiconductor to an *n*-type metal [12–14]. The crystal structure remains orthorhombic *Pbnm* up to $x = 0.3$, where it

* Corresponding author. Tel.: +1-352-846-0525; fax: +1-352-846-1182.

E-mail address: dnort@mse.ufl.edu (D.P. Norton).

becomes orthorhombic *Ibmm*. For $x > 0.7$, bulk $\text{La}_{1-x}\text{Sr}_x\text{TiO}_3$ becomes cubic.

Epitaxial film growth studies have explored the (La,Sr)TiO₃ system [15–19]. Using molecular beam epitaxy, it has been shown that phase formation in the LaTiO_x system can be controlled via selection of oxidation conditions and temperature during growth. The epitaxial growth of (La,Sr)TiO₃ thin films has also been examined using pulsed-laser deposition. La_{0.5}Sr_{0.5}TiO₃ films have been realized with resistivity on the order to 60 μΩ-cm at room temperature [19]. Interestingly, epitaxial La_{0.5}Sr_{0.5}TiO₃ thin films that are reasonably transparent and conductive have also been realized [20]. In this case, films with a resistivity of ~350 μΩcm were measured to possess a transparency of ~70% over the visible wavelengths.

As a metallic oxide, (La,Sr)TiO₃ is being considered for numerous applications, including conducting electrodes for ferroelectrics [21] and dielectric-base transistors [22], as well as for sensors [23]. Another potential application of (La,Sr)TiO₃ is in the development of coated conductors based on epitaxial high temperature superconducting (HTS) films deposited on metal tapes [24,25]. The growth of epitaxial HTS films on biaxially textured substrates eliminates high-angle grain boundaries and enables high superconducting currents. One particular approach based on the use of rolling assisted biaxially textured substrates (RABiTS) requires the growth of oxide buffer layers on biaxially textured metal surfaces [24]. These buffer layers must be epitaxial with respect to the biaxially textured metal tape, chemically robust, and suitable for subsequent superconductor film growth. The specific interest in conducting oxides for practical HTS conductors arises from the need to accommodate current flow in the event of a local supercurrent quenching event. Such an occurrence will lead to detrimental failure of the conductor if a critical value of power dissipation is exceeded. With the RABiTS process, an obvious approach to redirecting large current flow due to a local failure in the HTS film would be to shunt the current through the metallic substrate. However, this requires a continuous metallic interconnect between the HTS film and the normal metal substrate. A conducting buffer layer architecture would meet this requirement.

In functioning as a conducting buffer layer in an RABiTS structure, the conductive oxide layer architecture must satisfy a specific set of criteria [26]. First, the buffer layer must be reasonably well lattice matched to both the metal substrate and the superconducting film, thus enabling epitaxy. Second, the material must be conductive not only as deposited, but after subsequent HTS film growth and oxygen annealing. Third, the interaction between the buffer layer and the metal substrate must be such as to minimize formation of any native interfacial oxide that would serve as an insulating barrier to shunted current flow. Among the conducting

oxide materials, (La,Sr)TiO₃ appears to satisfy these criteria. At room temperature, LaTiO₃ possesses the orthorhombic GdFeO₃ perovskite structure with $a = 5.604 \text{ \AA}$, $b = 5.595 \text{ \AA}$, and $c = 7.906 \text{ \AA}$ [27]. The pseudo-cubic lattice parameter of 3.96 \AA provides a relatively large (12%) lattice mismatch to Ni ($a = 3.524 \text{ \AA}$), although similar mismatched parameters have proven useful in other RABiTS architectures [28–32]. La, Sr, and Ti have a high affinity for oxygen relative to Ni, suggesting that native NiO formation at the interface should be minimal.

In this paper, we examine the properties of (La,Sr)TiO₃ films relative to its use as a conductive buffer layer for coated conductor applications. First, the properties of (La,Sr)TiO₃ thin films as a function deposition conditions are examined, with a focus on elucidating the effectiveness of Sr doping in maintaining conductivity for films grown under oxidizing conditions. In particular, the conductivity of La_{0.5}Sr_{0.5}TiO₃ and LaTiO₃ films is measured and compared. The growth of (La,Sr)TiO₃ thin films was achieved using pulsed-laser deposition. A KrF (248 nm) excimer laser was used as the ablation source. Laser energy densities on the order of 1–3 J/cm² were utilized. Films were deposited at temperatures ranging from 500–770 °C in pressures ranging from vacuum (10⁻⁶ Torr) to oxygen partial pressures of 10⁻² Torr. Polycrystalline LaTiO₃ and La_{0.5}Sr_{0.5}TiO₃ targets were used as the ablation materials. Total deposition time was 0.5 to 1 h with a laser repetition rate of 5 Hz. In most cases, the films were rapidly cooled in the growth pressure following deposition. Single crystal (001) SrTiO₃, as well as biaxially-textured Ni and Ni–W alloy tapes (3 at.% W), were used as the substrate material. The substrates were cleaned in trichloroethylene, acetone, and methanol prior to loading in the growth chamber. The metal substrates were heated to the growth temperature in a 4% H₂/96% Ar ambient with a pressure of 100 mTorr. Prior to nucleation, the hydrogen was evacuated. For consistent growth of (001) oriented films, nucleation was performed in vacuum at ~650°C. After film growth, the films were cooled in vacuum. The transport and structural properties of both LaTiO₃ and La_{0.5}Sr_{0.5}TiO₃ thin films were characterized. Transport was determined at room temperature using a van der Pauw configuration. X-ray diffraction was used to determine crystallographic orientation and lattice spacing.

Fig. 1 shows the X-ray diffraction low-resolution 2θ scan for the LaTiO₃ film on (001) textured Ni. Based on the in-plane and high-resolution scans for films on textured metal and on single crystal SrTiO₃, the LaTiO₃ film was indexed as possessing two orientations, namely the LaTiO₃ (110) perpendicular or the LaTiO₃ (001) perpendicular. There is no evidence for an orthorhombic *a,b* splitting as has been reported for the bulk [27]. If the peaks along the surface normal are indexed as (001)

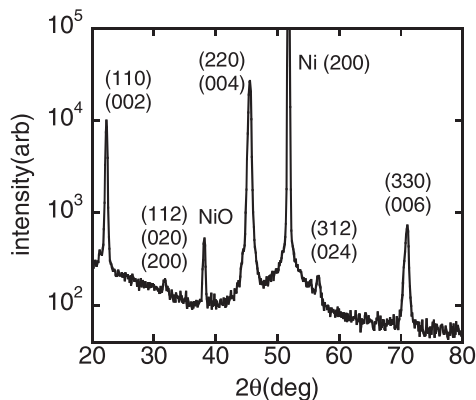


Fig. 1. X-ray diffraction θ - 2θ scans taken the surface normal for an LaTiO_3 film deposited on (001) biaxially textured Ni.

perpendicular, then the resulting tetragonal lattice parameters are $a = b = 5.594 \text{ \AA}$, $c = 7.880 \text{ \AA}$. For this orientation, the out-of-plane LaTiO_3 [001] is along the Ni[001], while the in-plane LaTiO_3 is along the Ni [110]. Alternatively, if the peaks along the surface normal are indexed as (110) perpendicular, then $a = b = 5.572 \text{ \AA}$, $c = 7.910 \text{ \AA}$. For this orientation, the out-of-plane LaTiO_3 [110] is along the Ni [001], while the in-plane LaTiO_3 [001] is along the Ni [100]. The two sets of lattice values are related by interchanging (a, b) with c and scaling by $\sqrt{2}$. Both orientations exist in the film with comparable volume fraction. Fig. 2 shows the rocking curves for the LaTiO_3 (004)/(220) and the (002) Ni substrate peaks. The out-of-plane mosaic spread for the LaTiO_3 film of $\Delta\theta \sim 3.7^\circ$ is significantly narrower than that for the biaxially textured substrates, measured in this case to be $\Delta\theta \sim 9.7^\circ$. This has been observed for other epitaxial oxides on biaxially textured metal substrates. The improved alignment of the film surface normal axis relative to the crystallinity of the substrate reflects the influence of surface energy in determining the surface normal of the film. Ironically, a larger lattice mismatch between film and substrate appears to increase this influence of surface energy in orienting the film crystallinity, thus leading to a narrower out-of-plane mosaic relative to the substrate. Fig. 3 shows the in-plane φ -scans for the LaTiO_3 film and Ni substrate. The presence of only three in-plane peaks in the φ -scan through the LaTiO_3 (112) reflects the measurement procedure in which the scan was performed over a φ -angle range of 300° . A wider scan over 360° would have revealed a fourth peak. The full-width half-maximum for the film peaks is $\Delta\varphi \sim 9.6^\circ$ is slightly smaller than that in the substrate. While the epitaxial growth of LaTiO_3 on (001) Ni has clearly been achieved, the stability of the LaTiO_3/Ni interface is limited to low oxygen conditions due to the phase transitions that occur with increased oxygen content.

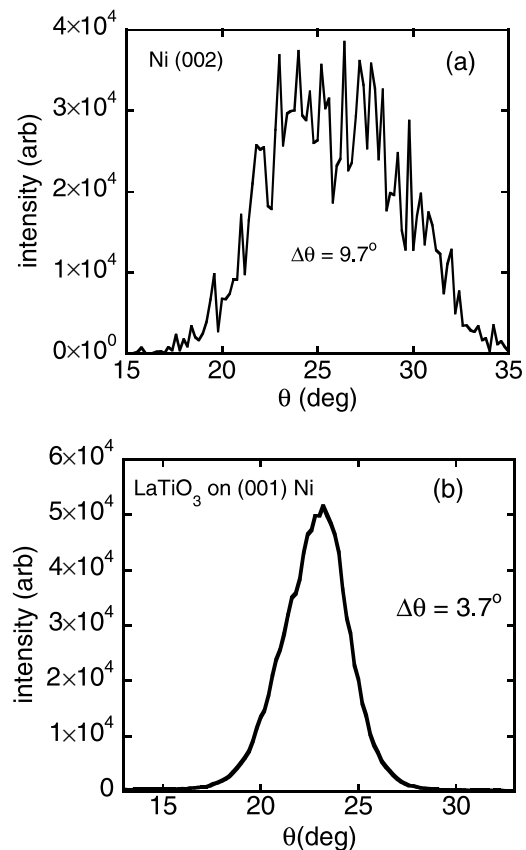


Fig. 2. Rocking curve for: (a) the biaxially textured Ni substrate and (b) epitaxial LaTiO_3 film.

In addition to studying the epitaxial growth of $(\text{La,Sr})\text{TiO}_3$ on biaxially textured (001) Ni and Ni alloys, the structural and transport properties of the $(\text{La,Sr})\text{TiO}_3$ films on single crystal (001) SrTiO_3 substrates were also investigated. Epitaxial structures grown on (001) SrTiO_3 substrates were used to evaluate fundamental transport and structure properties. Both the structural and transport properties of the LaTiO_{3+x} films were dependent on the oxidizing environment utilized during growth. Fig. 4 shows the behavior of the LaTiO_3 (004) peak as a function of oxygen pressure during growth. The data indicates a discontinuous change in c -axis spacing from 3.978 \AA for films deposited in vacuum to 4.200 \AA for films deposited at 10^{-3} Torr. This change in c -axis spacing is consistent with the insertion of additional oxygen atoms within intergrowths as seen in bulk studies. For comparison, the structure of $\text{La}_{0.5}\text{Sr}_{0.5}\text{TiO}_3$ films were also examined as a function of film growth conditions. In contrast to the LaTiO_3 , no significant shift in c -axis lattice spacing could be detected using low resolution X-ray diffraction. Fig. 4b shows the diffraction data for the (004) $(\text{La,Sr})\text{TiO}$ peak for films grown at different O_2 pressures. The lattice

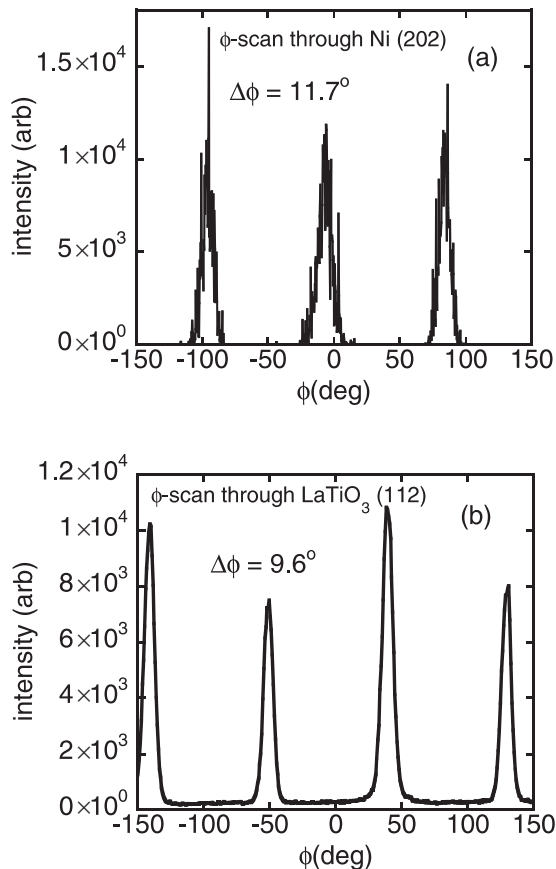


Fig. 3. X-ray diffraction ϕ -scan for: (a) the biaxially textured Ni substrate and (b) epitaxial LaTiO_3 film.

spacing is essentially unchanged from that for the film grown in vacuum.

The transport behavior of epitaxial $(\text{La,Sr})\text{TiO}_3$ films grown on SrTiO_3 is indicated in Fig. 5, where the room temperature resistivity is plotted as a function of oxygen pressure during growth. For films grown in vacuum, the resistivity for both LaTiO_3 and $\text{La}_{0.5}\text{Sr}_{0.5}\text{TiO}_3$ epitaxial films grown in vacuum is low and nearly identical, with a resistivity on the order of $10^{-4} \Omega\text{cm}$. This plot is for films grown at 750°C . As the oxygen partial pressure is increased to 10^{-4} Torr, the resistivity of the LaTiO_3 film increases by more than two orders of magnitude to $\sim 0.026 \Omega\text{cm}$. At 10^{-3} Torr, the resistivity is $0.26 \Omega\text{cm}$. This increase in resistivity with oxygen pressure during growth correlates with a structural transition as is evident in the X-ray diffraction patterns shown in Fig. 4. In contrast, the resistivity of the $\text{La}_{0.5}\text{Sr}_{0.5}\text{TiO}_3$ films is relatively insensitive to oxygen partial pressure during growth. As seen in Fig. 5, the resistivity of $\text{La}_{0.5}\text{Sr}_{0.5}\text{TiO}_3$ films varies little as a function of oxygen pressure, increasing from $1 \times 10^{-4} \Omega\text{cm}$ when deposited in vacuum to $3 \times 10^{-4} \Omega\text{cm}$ at a partial

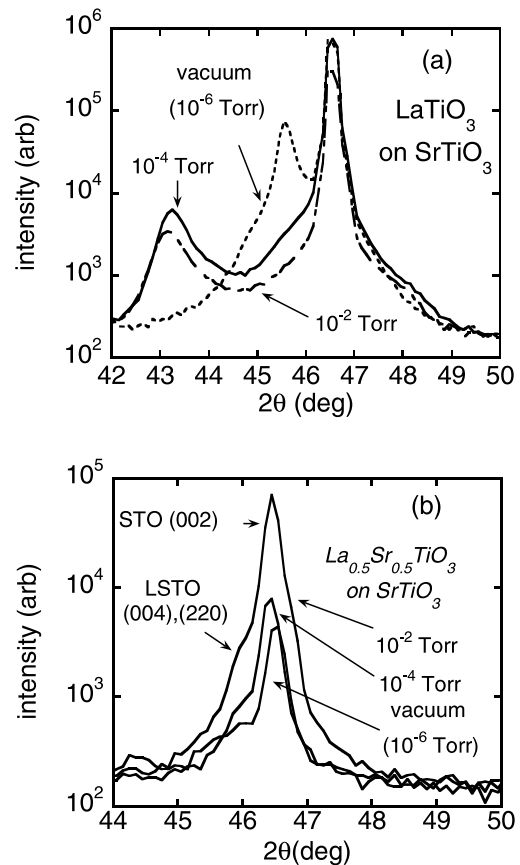


Fig. 4. X-ray diffraction scans for: (a) epitaxial LaTiO_3 and (b) epitaxial $\text{La}_{0.5}\text{Sr}_{0.5}\text{TiO}_3$ films grown on (001) SrTiO_3 at 750°C in various oxygen pressures.

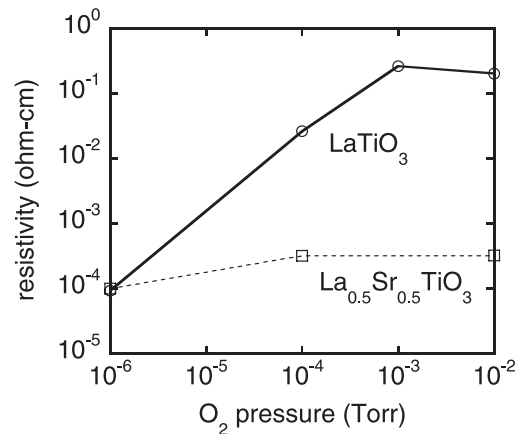


Fig. 5. Resistivity for LaTiO_3 and $(\text{La,Sr})\text{TiO}_3$ films grown at various oxygen pressures.

pressure of 10^{-4} to 10^{-2} Torr. As seen in the figure, the transport properties of LaTiO_{3+x} are quite sensitive to

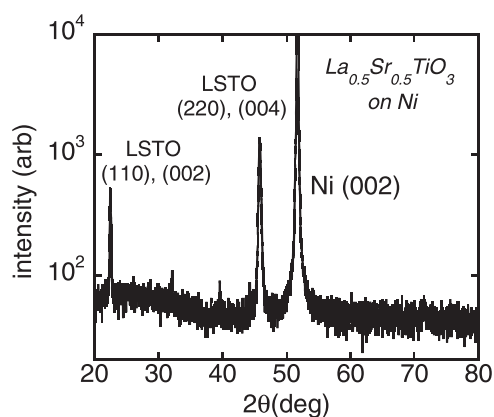


Fig. 6. X-ray diffraction θ - 2θ scans taken the surface normal for a $\text{La}_{0.5}\text{Sr}_{0.5}\text{TiO}_3$ film deposited on (001) biaxially textured Ni.

oxygen content, thus making it unattractive as a conductive buffer for RABiTS applications. However, the addition of Sr to LaTiO_3 should assist in maintaining metallic conductivity under oxidizing conditions. Fig. 6 shows the X-ray diffraction data for a $\text{La}_{0.5}\text{Sr}_{0.5}\text{TiO}_3$ film grown on the Ni-W biaxially textured alloy substrate. The film was grown at 650°C in vacuum ($\sim 10^{-6}$ Torr). The film is epitaxial and c -axis oriented.

In conclusion, we have investigated the transport and structural properties of LaTiO_3 and $\text{La}_{0.5}\text{Sr}_{0.5}\text{TiO}_3$ epitaxial thin films grown by pulsed laser deposition. Epitaxy was achieved on biaxially-textured Ni and Ni alloy substrates. Transport measurements show that Sr-doping of LaTiO_3 thin films is effective in stabilizing the conducting properties when exposed to oxidizing conditions at elevated temperatures. Future efforts will address the growth of HTS films on these material, and the subsequent conductivity of the layers with subjected to high pressure anneals needed to optimal HTS properties.

Acknowledgements

This work was supported through a contract with Oak Ridge National Laboratory, which is managed by UT/Battelle under US Government contract DE-AC05-00OR22725, as well as from the Air Force Office of Scientific Research.

References

- [1] Ginley DS, Bright C. MRS Bull 2000;25:15.
- [2] Goodenough JB. Metallic oxides. In: Progress in solid state chemistry, vol. 5. Oxford: Pergamon Press; 1971. p. 145–399.
- [3] Cox PA. Transition metal oxides. Oxford: Clarendon Press; 1995.
- [4] Tokura Y. Physica B 1997;237–238:1.
- [5] Khaliullin G, Maekawa S. Phys Rev Lett 2000;85:3950.
- [6] Keimer B, Casa D, Ivanov A, Lynn JW, Zimmermann Mv, Hill JP, et al. Phys Rev Lett 2000;85:3946.
- [7] Bednorz JG. Physica C 1997;282–287:37.
- [8] Miyahara S, Mila F. Progress of Theoretical Physics 2002;145:266 [supplement issue].
- [9] Lichtenberg F, Widmer D, Bednorz JG, Williams T, Reller A. Z Phys B 1991;82:211.
- [10] Williams T, Lichtenberg F, Widmer D, Bednorz JG, Reller A. J Solid State Chem 1993;103:375.
- [11] Nanamatsu S, Kimura M, Doi K, Matsushita S, Yamada N. Ferroelectrics 1974;8:511.
- [12] Hays CC, Zhou JS, Markert JT, Goodenough JB. Phys Rev B 1999;60:10367.
- [13] Tokura Y, Taguchi Y, Okada Y, Fujishima Y, Arima T, Kumagai K, et al. Phys Rev Lett 1993;70:2126.
- [14] Maeno Y, Awaji S, Matsumoto H, Fujita T. Physica B 1990;165–166(Part 2):1185.
- [15] Seo JW, Fompeyrine J, Siegwart H, Locquet J-P. Phys Rev B 2001;63:205401/1-7.
- [16] Ohtomo A, Muller DA, Grazul JL, Hwang HY. Appl Phys Lett 2002;80:3922.
- [17] Gariglio S, Seo JW, Fompeyrine J, Locquet J-P, Triscone J-M. Phys Rev B 2001;63:161103/1-4.
- [18] Yoshida C, Tamura H, Yoshida A, Kataoka Y, Fujimaki N, Yokoyama N. Jap J Appl Phys 1996;35:5691.
- [19] Wu W, Lu F, Wong KH, Pang G, Choy CL, Zhang Y. J Appl Phys 2000;88:700.
- [20] Cho JH, Cho HJ. Appl Phys Lett 2001;79:1426.
- [21] Liu BT, Maki K, So Y, Nagarajan V, Ramesh R, Lettieri J, et al. Appl Phys Lett 2002;80:4801.
- [22] Hato T, Yoshida A, Yoshida C, Suzuki H, Yokoyama N. Appl Phys Lett 1997;70:2900.
- [23] Li GQ, Lai PT, Zeng SH, Huang MQ, Cheng YC. Sensors Actuata A 1997;63:223.
- [24] Norton DP, Goyal A, Budai JD, Christen DK, Kroeger DM, Specht ED, et al. Science 1996;274:755.
- [25] Wu XD, Foltyn SR, Arendt PN, Blumenthal WR, Campbell IH, Cotton JD, et al. Appl Phys Lett 1995;67:2397.
- [26] Cantoni C, Aytug T, Verebelyi DT, Paranthaman M, Specht ED, Norton DP, et al. IEEE Trans Appl Supercond 2001;11:3309.
- [27] Yoshii K, Nakamura A, Abe H. J Alloys Compd 1999; 290:236.
- [28] Donet S, Weiss F, Senateur JP, Chaudouet P, Abrutis A, Teiserskis A, et al. J Phys 2001;11(11):P319–23, IV (Proceedings).
- [29] de Boer B, Reger N, Fernandez G-R, Eickemeyer J, Holzapfel B, Schultz L, et al. Physica C 2001;351:38.
- [30] Goyal A, Feenstra R, List FA, Paranthaman M, Lee DF, Kroeger DM, et al. JOM 1999;51:19.
- [31] Parilla PA, Carlson CM, Wang Y-T, Bhattacharya RN, Blaugher RD, Ginley DS, et al. IEEE Trans Appl Supercond 1999;9:1673.
- [32] Lee DE, Paranthaman M, Mathis JE, Goyal A, Kroeger DM, Specht ED, et al. Jpn J Appl Phys 1999;38:L178.